Cell, Volume *139*

Supplemental Data

Induction of Intestinal Th17 Cells

by Segmented Filamentous Bacteria

Ivaylo I. Ivanov, Koji Atarashi, Nicolas Manel, Eoin L. Brodie, Tatsuichiro Shima, Ulas Karaoz, Dongguang Wei, Katherine C. Goldfarb, Clark A. Santee, Susan V. Lynch, Takeshi Tanoue, Akemi Imaoka, Kikuji Itoh, Kiyoshi Takeda, Yoshinori Umesaki, Kenya Honda, and Dan R. Littman

Supplemental Experimental Procedures

PhyloChip Methods

Nucleic acid extraction from mouse small intestines. Distal halves of the small intestine from 4 mice from each group were dissected, flash frozen in liquid nitrogen and stored at -80ºC. For extraction, each frozen gut section was transferred with sterile forceps to a 2 mL Lysing Matrix E tube (MP Biomedicals) containing 50 µL of 0.1M aluminum ammonium sulfate. Equal volumes (500 µL) of modified CTAB buffer (10% CTAB, 250 mM phosphate, 300 mM NaCl) and phenol:chloroform:isoamylalcohol (25:24:1) were added to each tube, tubes were agitated with a FastPrep (MP Biomedicals: 30 seconds, 5.5 m/s) and centrifuged (5 min, 4ºC, 16,000 x *g*). Aqueous phases were removed by pipette, transferred to phase-lock gel tubes (MaXtract High Density Gel Tubes, Qiagen) containing approximately 1 aqueous volume of chloroform, inverted by hand and centrifuged again to yield a crude nucleic acid extract. Another 500 µL aliquot of modified CTAB buffer was added to the Lysing Matrix E tube and tubes were agitated and centrifuged again as described above. This second aqueous extract was purified with chloroform as above to yield an additional crude nucleic extract. This re-extraction step was repeated twice. Each of the three crude nucleic acid extracts from a sample was transferred from the phase-lock gel tube to an individual 2 mL tube, gently mixed by pipette with 2 volumes of polyetheleneglycol/salt solution (30% wt/vol PEG 6000, 1.6M NaCl), and incubated at room temperature for 2 hours. Crude nucleic acid extracts were then centrifuged (10 min, 4ºC, 16,000 x *g*), supernatants were removed by pipette and pellets were washed with 1 mL ice-cold 70% ethanol. Pellets were resuspended in 60 µL of nuclease-free (DEPC treated) water. The three crude nucleic acid extracts from each sample were combined and a 60 µL aliquot was purified by column chromatography using an DNA/RNA Allprep Kit (Qiagen, CA). DNA and RNA were separately eluted and purified. Purified DNA was eluted in 2 x 25 µL Buffer EB and used as genomic DNA template for PCR amplification.

PCR amplification of 16S rRNA genes. Genomic DNA from the eight samples was quantified by NanoDrop1000, and diluted in nuclease-free water to achieve a standard concentration of 500 ng/µL. Eight replicate polymerase chain reactions were prepared for each gut sample containing final concentrations of 10 ng/µL gDNA template, 0.02 U/µL ExTaq (Takara Bio Inc.), 1X ExTaq buffer, 0.2 mM dNTP mixture, 1µg/µL Bovine Serum Albumin (BSA), and 300 pM each of universal bacterial primers: 27F (5'-AGAGTTTGATCCTGGCTCAG-3') and 1492R (5'-GGTTACCTTGTTACGACTT-3'). To minimize PCR bias due to variable template annealing efficiencies and random effects, PCR was performed on a BioRad iCycler with an eight temperature annealing gradient (48-58˚C) and the following conditions: 95˚C (3 min), followed by 30 cycles of 95˚C (30 sec), annealing (30 sec), 72˚C (2 min), and a final extension at 72˚C (10 min). Reactions were combined for each sample and concentrated with 0.8

volumes isopropanol, washed twice with ice cold 70% ethanol and resuspended in 50 µL nuclease-free water.

PhyloChip microarray analysis of 16S rRNA gene diversity. 500 ng of pooled PCR amplicons of each sample were spiked with known concentrations of amplicons derived from yeast and bacterial metabolic genes. This mix was fragmented to 50–200 bp using DNase I (0.02 U μg^{-1} DNA, Invitrogen, Carlsbad, CA, USA) and One-Phor-All buffer (GE Healthcare, Piscataway, NJ, USA) following the manufacturer's protocols. The mixture was then incubated at 25 °C for 20 min and 98 °C for 10 min before biotin labeling with a GeneChip DNA labeling reagent kit (Affymetrix, Santa Clara, CA, USA) following the manufacturer's instructions. Next, the labeled DNA was denatured at 99 °C for 5 min and hybridized to custom-made Affymetrix GeneChips (16S rRNA genes PhyloChips) at 48 °C and 60 rpm for 16 h. PhyloChip washing and staining were performed according to the standard Affymetrix protocols described previously (Masuda and Church 2002).

Each PhyloChip was scanned and recorded as a pixel image, and initial data acquisition and intensity determination were performed using standard Affymetrix software (GeneChip microarray analysis suite, version 5.1). Background subtraction, data normalization and probe pair scoring were performed as reported previously (DeSantis, Hugenholtz et al. 2006; Brodie, Desantis et al. 2007; DeSantis, Brodie et al. 2007). The positive fraction (PosFrac) was calculated for each probe set as the number of positive probe pairs divided by the total number of probe pairs in a probe set. Taxa were deemed present when the PosFrac value exceeded 0.90. Intensities were summarized for each taxon/probe-set using a trimmed average (highest and lowest values removed before averaging) of the intensities of the perfect match probes (PM) minus their corresponding mismatch probes (PM).

Normalization of PhyloChip data of bacterial community composition. To correct for variation associated with quantification of amplicon target (quantification variation), and downstream variation associated with target fragmentation, labeling, hybridization, washing, staining and scanning (microarray technical variation), a two-step normalization procedure was developed.

First, for each PhyloChip experiment, a scaling factor best explaining the intensities of the spiked control probes under a multiplicative error model was estimated using a maximum-likelihood procedure as follows. PhyloChip design contains control probes targeting amplicons of bacterial metabolic genes and synthetic 16S rRNA genes (spike-in probes). These are spiked in known quantities into the final hybridization mix. To take advantage of the spiked probesets, an optimization procedure similar to the one suggested in (Hartemink, Gifford et al. 2001) was implemented in R software environment (http://www.r-project.org).

Assume that for a dataset of A PhyloChips, the measured intensities of B spike-in probesets are summarized in a data matrix, where an element x_{ab} corresponds to the measured intensity of probeset b in PhyloChip a. Let t_b denote the true expression level of the probeset b. Due to variation introduced during fragmentation, biotinylation, hybridization, staining, and scanning steps as well as due to the batch-to-batch variability between the chips, the measured expression levels (x_{ab}'s) will differ from the true expression levels. In our model, these error components are assumed to be multiplicative implying that the actual levels of the true intensities will affect the measured intensities. Under these assumptions, the measured intensity of probeset b in PhyloChip a (x_{ab}) can be expressed as a product of the true intensity (t_b) with a chip specific error factor m_a and a random error e_{ab}:

$$x_{ab} = t_b \times m_a \times e_{ab}$$

Log transformation results in an additive error model:

$$\log(x_{ab}) = \log(t_b) + \log(m_a) + \log(e_{ab})$$

We assume the random noise component to be Gaussian distributed with zero mean and a probeset specific variance (σ_b^2). This makes the (log) measured expression levels Gaussian distributed with mean $\log(t_b) + \log(m_a)$ and variance σ_b^2:

$$\log(x_{ab}) \sim N\left(\log(t_b) + \log(m_a), \sigma_b^2\right)$$

For all a and b, let $y_{ab} = \log(x_{ab})$, $\mu_b = \log(t_b)$, and $\alpha_a = \log(m_a)$. Under this Gaussian model, the log-likelihood L of observing the measured spike intensities can be expressed as follows:

$$\begin{aligned} L &= \log\left(\prod_{b=1}^{\substack{\#\,spike-in\\ probesets}} \prod_{a=1}^{\#\,experiments} P\left(y_{ab} \mid \mu_b, \alpha_a, \sigma_b^2\right) \right) \\ &= \sum_{b=1}^{\substack{\#\,spike-in\\ probesets}} \sum_{a=1}^{\#\,experiments} -\frac{1}{2}\left[\log\left(2\pi\sigma_b^2\right) + \frac{\left(y_{ab} - \mu_b - \alpha_a\right)^2}{\sigma_b^2} \right] \end{aligned}$$

To find the optimal scaling factors for each experiment, we solve for the values of $\mu_b, \alpha_a,$ and σ_b^2 that maximize the log-likelihood function denoted as $\hat{\mu}_b, \hat{\alpha}_a,$ and $\hat{\sigma}_b^2$. Using R, we implemented the iterative optimization procedure to compute the $\hat{\alpha}_a$'s for each of the experiments. Using these, the optimal scaling factor for PhyloChip a can be expressed as:

$$s_a = \frac{1}{\hat{m}_a} = e^{-\hat{\alpha}_a}$$

In the first normalization step, the intensities in each experiment are multiplied with its corresponding optimal scaling factor.

For the second step of normalization, the intensities for each experiment are corrected for the variation in total array intensity by dividing the intensities by its corresponding total array intensity for bacterial probe sets. The normalized data is available in Table S1.

Statistical Analysis of PhyloChip data of bacterial community composition. Following normalization and scaling, microarray intensity data was log transformed. For comparison of bacterial community structure between samples, only those bacterial taxa detected in at least 3 out of 4 replicates from either supplier of mouse were considered. A distance matrix was calculated using the trimmed average fluorescence intensity data using the Bray-Curtis distance metric within the function 'vegdist' in the R package 'vegan'. The distance matrix was represented as a dendrogram with average-linkage using the function 'hclust'. To determine organisms that varied significantly in relative abundance between the mice from the two suppliers we applied a two-sample t-test (assuming unequal variances). The raw pvalues were corrected for multiple testing using Benjamini-Hochberg procedure. The mean number of

16S rRNA gene molecules in each hybridization was estimated for Jackson and Taconic groups based on spiked control probes using a linear fit of normalized intensities to the log number of molecules applied. A comparison of fold-difference in intestinal bacterial relative abundance between Taconic and Jackson mice is available in Table S2.

Phylogenetic tree construction. A phylogenetic tree was generated using representative 16S rRNA sequences for those bacterial taxa detected in at least 3 out of 4 replicates from either supplier of mice and displaying significant differences in relative abundance between suppliers. Representative sequences were exported aligned (7682 character NAST alignment (DeSantis, Hugenholtz et al. 2006)) from the greengenes database (DeSantis, Hugenholtz et al. 2006) and local bootstrapped neighbor joining trees constructed using FastTree (Price, Dehal et al. 2009) with default settings. Dendrograms were annotated using the Interactive Tree of Life (ITOL) web server (http://itol.embl.de/) (Letunic and Bork 2007).

Phylogenetic analysis of SFB-related bacteria was performed in ARB (Ludwig, Strunk et al. 2004) with trees generated using maximum likelihood (AxML) with hypervariable regions excluded using the Lane Mask.

Fecal DNA Extraction for qPCR

Bacterial genomic DNA was extracted from fresh or frozen fecal samples (within an experiment the samples were treated identically) by phenol-chloroform extraction. Briefly ~100mg of fecal sample was suspended in a solution containing 500 µl of DNA extraction buffer, 210 µl of 20% SDS, 500 µl of a mixture of of phenol:chloroform:isoamyl alcohol (25:24:1), and 500 µl of a slurry of 0.1-mm-diameter zirconia/silica beads (BioSpec Products, Bartlesville, OK). Cells were lysed by mechanical disruption with a FastPrep bead beater set on high for 45 sec, after which three rounds of phenol:chloroform extraction were performed. DNA was resuspended in TE buffer with 100 µg/ml RNase.

RT-PCR Primer Sequences

Primers for IL-17A, IL-17F, IL-21, IL-22, RORγt and GAPDH have been described previously (Atarashi, Nishimura et al. 2008). The following primer sets were also used: SAA1, 5'-CATTTGTTCACGAGGCTTTCC-3' and 5'-GTTTTTCCAGTTAGCTTCCTTCATGT-3'; SAA2, 5'-TGTGTATCCCACAAGGTTTCAGA-3' and 5'-TTATTACCCTCTCCTCCTCAAGCA-3'; SAA3, 5'-CGCAGCACGAGCAGGAT-3' and 5'-CCAGGATCAAGATGCAAAGAATG-3'; NOS2, 5'-TGCCCCTTCAATGGTTGGT-3' and 5'-TCCTTCGGCCCACTTCCT-3'; Reg3g, 5'-CCTTCCTCTTCCTCAGGCAAT-3' and 5'-TAATTCTCTCTCCACTTCAGAAATCCT-3'; MMP7, 5'-ATCAGTGGGAACAGGCTCAGA-3' and 5'-TTGTCCACTAGACTATTGACCTTCTTTG-3'; and CCR6, 5'-TTGGTTCGCCACTCTAATCAGTAG-3' and 5'-GCAGTTCAGCCACACTCTCACT-3'.

Electron Microscopy

Dissected 0.5 cm pieces of the terminal ileum were cut open, fixed in fixative containing 2.5% glutaraldehyde and 2% paraformaldehyde in 0.1M sodium cacodylate buffer (pH 7.2) for 2 hours and post-fixed with 1% osmium tetroxide for 1.5 hours at room temperature, then processed in a standard manner and embedded in EMbed 812 (Electron Microscopy Sciences, Hatfield, PA) for transmission electron microscopy (TEM) or critical point dried for scanning electron microscopy (SEM). For TEM, semi-thin sections were cut at 1000 nm and stained with 1% Toluidine Blue to evaluate the quality of preservation. Ultrathin sections (60 nm) were cut, mounted on copper grids and stained with uranyl acetate and lead citrate by standard methods. Stained grids were examined using a Philips CM-12 electron microscope (FEI; Eindhoven, The Netherlands) and photographed with a Gatan (4k x2.7k) digital camera (Gatan, Inc., Pleasanton, CA). For SEM, critical point dried samples were quickly transferred to the SEM chamber to avoid contamination. No conductive coating was applied.

Supplemental References

Atarashi, K., J. Nishimura, et al. (2008). "ATP drives lamina propria T(H)17 cell differentiation." Nature **455**(7214): 808-12.

Brodie, E. L., T. Z. Desantis, et al. (2007). "Urban aerosols harbor diverse and dynamic bacterial populations." Proc Natl Acad Sci U S A **104**(1): 299-304.

DeSantis, T. Z., E. L. Brodie, et al. (2007). "High-density universal 16S rRNA microarray analysis reveals broader diversity than typical clone library when sampling the environment." Microb Ecol **53**(3): 371-83.

DeSantis, T. Z., P. Hugenholtz, et al. (2006). "Greengenes, a chimera-checked 16S rRNA gene database and workbench compatible with ARB." Applied and Environmental Microbiology **72**(7): 5069-5072.

DeSantis, T. Z., Jr., P. Hugenholtz, et al. (2006). "NAST: a multiple sequence alignment server for comparative analysis of 16S rRNA genes." Nucleic Acids Res **34**(Web Server issue): W394-9.

Hartemink, A., D. Gifford, et al. (2001). Maximum Likelihood Estimation of Optimal Scaling Factors for Expression Array Normalization. Microarrays: Optical Technologies and Informatics, SPIE. B. M., C. Y., D. A. and D. E. **4266:** 132–140.

Letunic, I. and P. Bork (2007). "Interactive Tree Of Life (iTOL): an online tool for phylogenetic tree display and annotation." Bioinformatics **23**(1): 127-8.

Ludwig, W., O. Strunk, et al. (2004). "ARB: a software environment for sequence data." Nucleic Acids Research **32**(4): 1363-1371.

Masuda, N. and G. M. Church (2002). "Escherichia coli gene expression responsive to levels of the response regulator EvgA." J Bacteriol **184**(22): 6225-34.

Price, M. N., P. S. Dehal, et al. (2009). "FastTree: computing large minimum evolution trees with profiles instead of a distance matrix." Mol Biol Evol **26**(7): 1641-50.

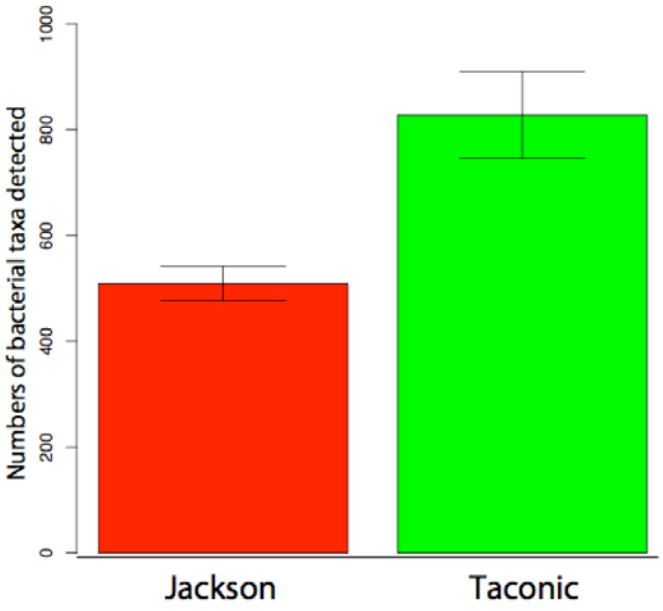

Figure S1. Bacterial Taxa in Jackson and Taconic C57BL/6 mice
Comparison of richness (number of passing bacterial taxa) between Jackson and Taconic mice. Jackson mice contain significantly (p=0.03) fewer bacterial taxa than Taconic.

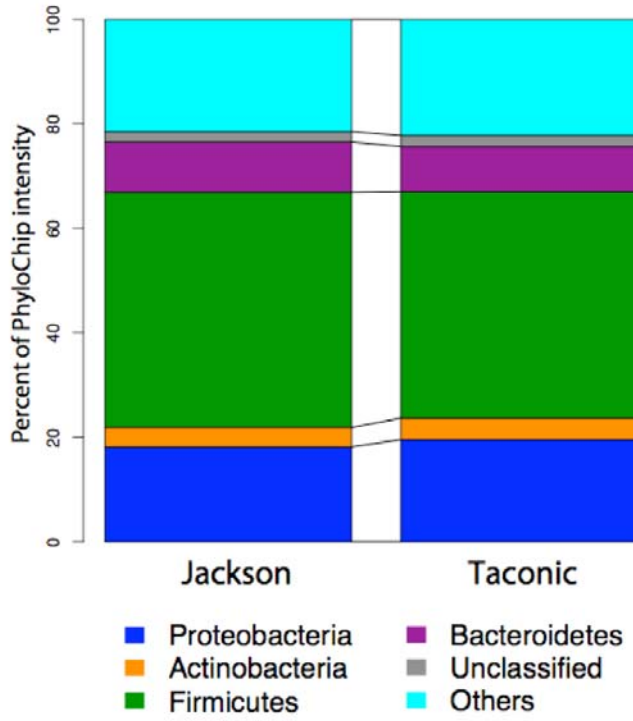

Figure S2. Comparison of relative abundances of major phyla between Jackson and Taconic mice
Overall the relative abundance of most phyla do not change between mouse suppliers apart from a small decrease in the Firmicutes and Bacteroidetes in Taconic and a corresponding increase in the relative abundance of the Proteobacteria. These differences are not statistically significant.

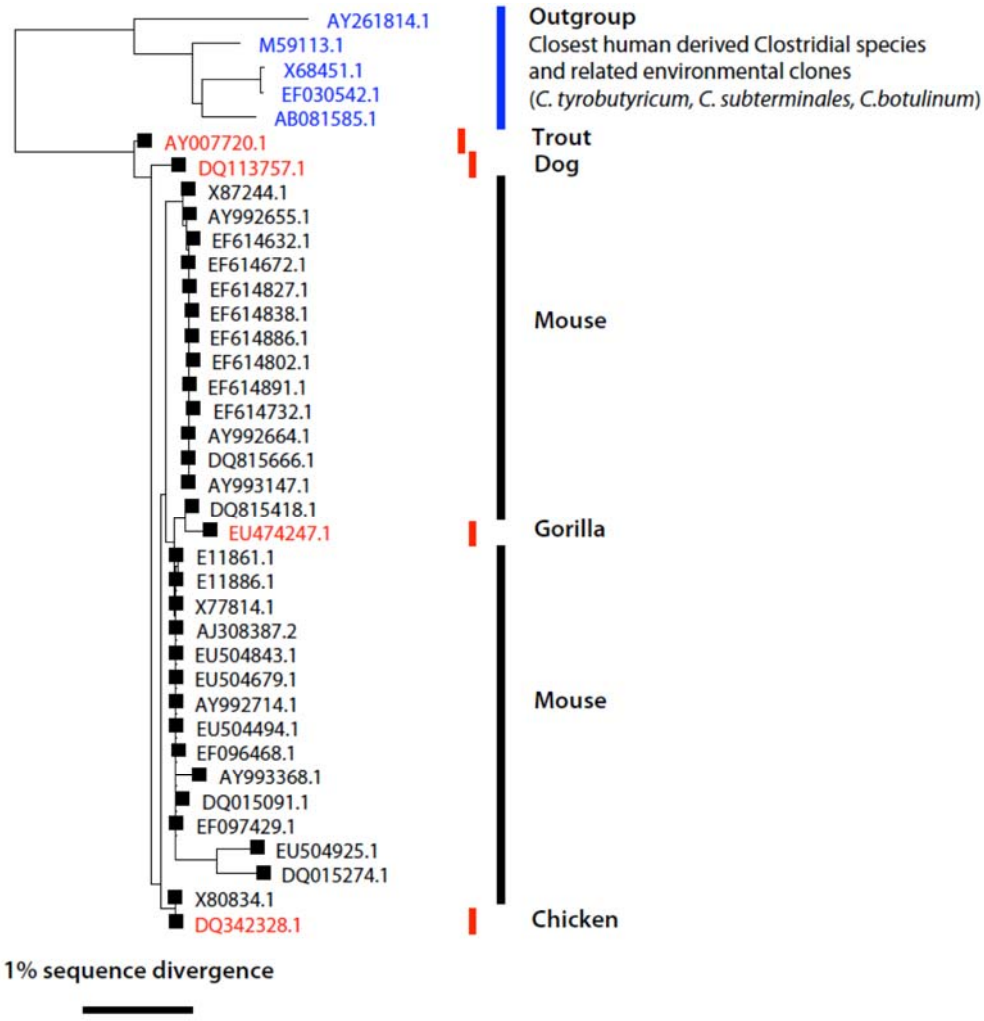

Figure S3. SFB-like bacteria in different hosts
Phylogenetic tree displaying the phylogenetic relationships between SFB-like bacteria detected in a number of hosts.

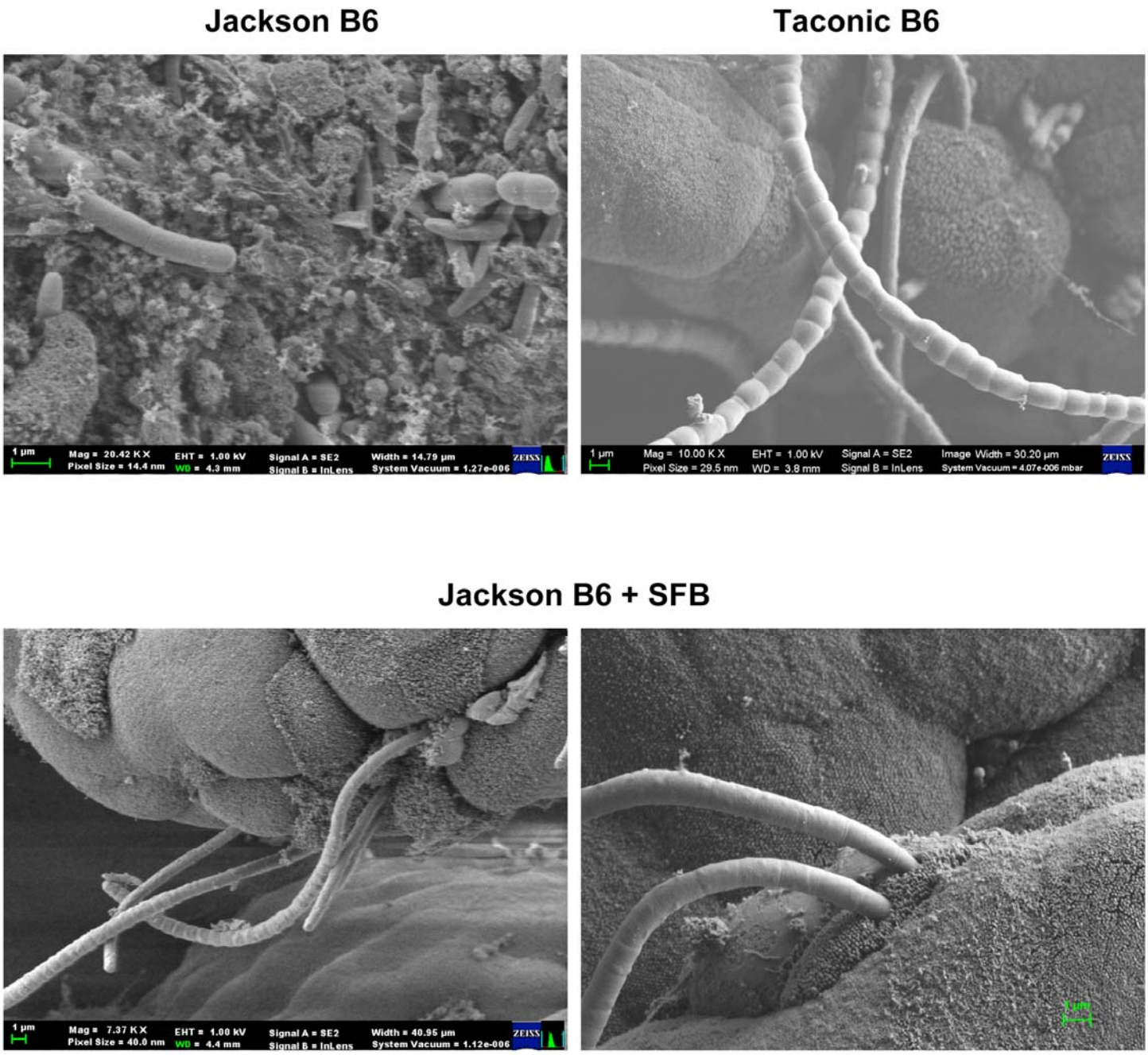

Figure S4. Bacterial morphology in the gut
High magnification SEM of terminal ileum showing non-SFB bacteria in Jackson B6 mice (top left panel) and SFB bacteria in Taconic B6 mice (top right panel). Upon co-housing with Taconic mice, SFB colonize the terminal ileum of Jackson mice (bottom left panel), where they adhere tightly to the epithelial cells (bottom right panel).

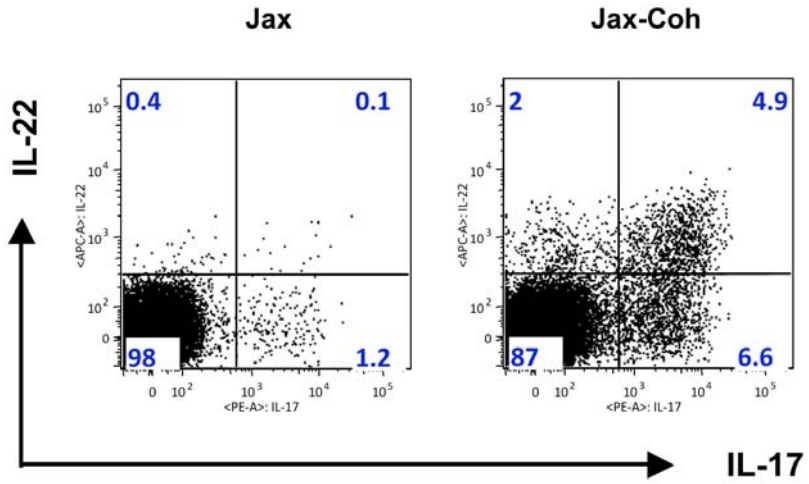

Figure S5. Co-housing of Jackson B6 mice with Taconic B6 mice induces Th17 cell differentiation 6 week old Jackson B6 and Taconic B6 females were placed in the same cage for 10 days, after which time LPL from the small intestine were isolated as described in Methods and analyzed for IL-17 and IL-22 expression. Plots from two animals gated on $TCR\beta^{+}CD4^{+}$ lymphocytes are presented. Data representative of numerous experiments.

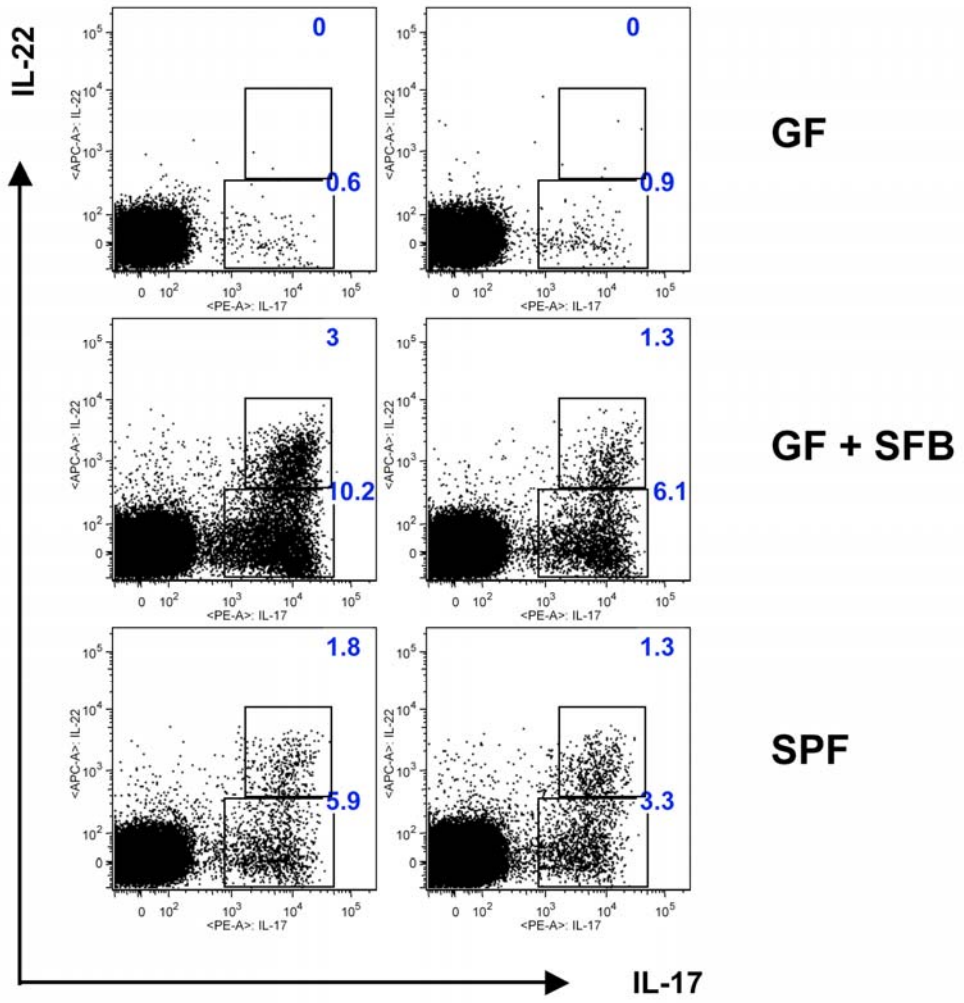

Figure S6. SFB induce Th17 cells in the large intestinal (LI) lamina propria (LP)
6 week old Swiss-Webster germ-free (GF) mice were colonized with SFB from feces of SFB-mono mice as described in Methods. LI LPL were prepared 13 days later and analyzed for intracellular cytokines. Each plot represents a separate animal. Plots gated on $TCR\beta^{+}CD4^{+}$ lymphocytes. One of several experiments is shown.

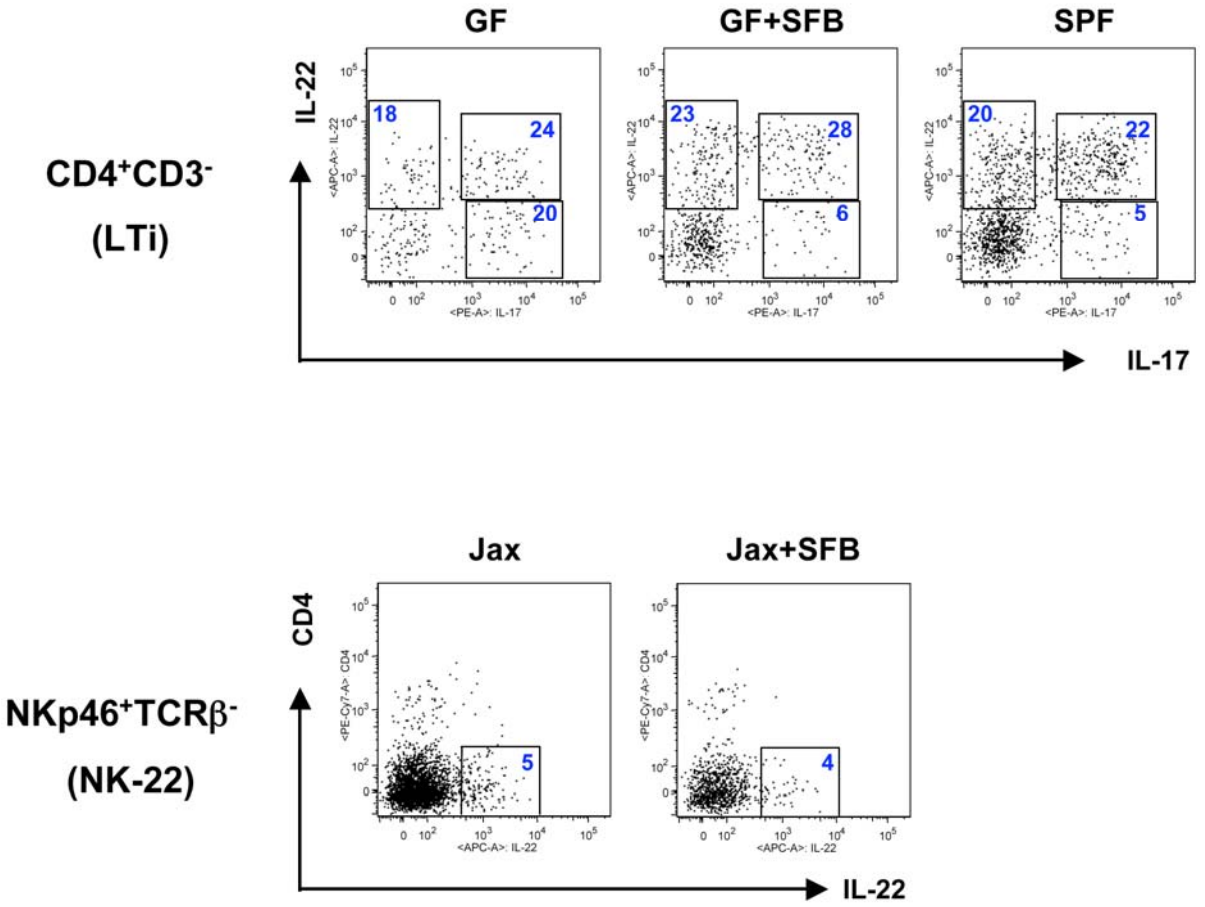

Figure S7. SFB colonization does not change IL-17 and IL-22 expression in non-T cells
(Top panels). IL-17 and IL-22 expression in $CD4^+CD3^-$ LTi-like cells in the SI LP. 6 week old Swiss-Webster mice were colonized with SFB from feces of SFB-mono mice and SI LPL isolated 10 days later. Plots represent individual mice and are gated on $CD4^+CD3^-$ cells. Representative data from numerous animals and experiments.
(Bottom panels) IL-22 expression in NKp46+ NK-22 cells in the SI LP. Jackson B6 mice were colonized with SFB for 14 days and SI LPL isolated as described in Methods. Plots represent individual mice and are gated on $NKp46^+TCR\beta^-$ cells. Representative data from one experiment with 3 mice in each group.

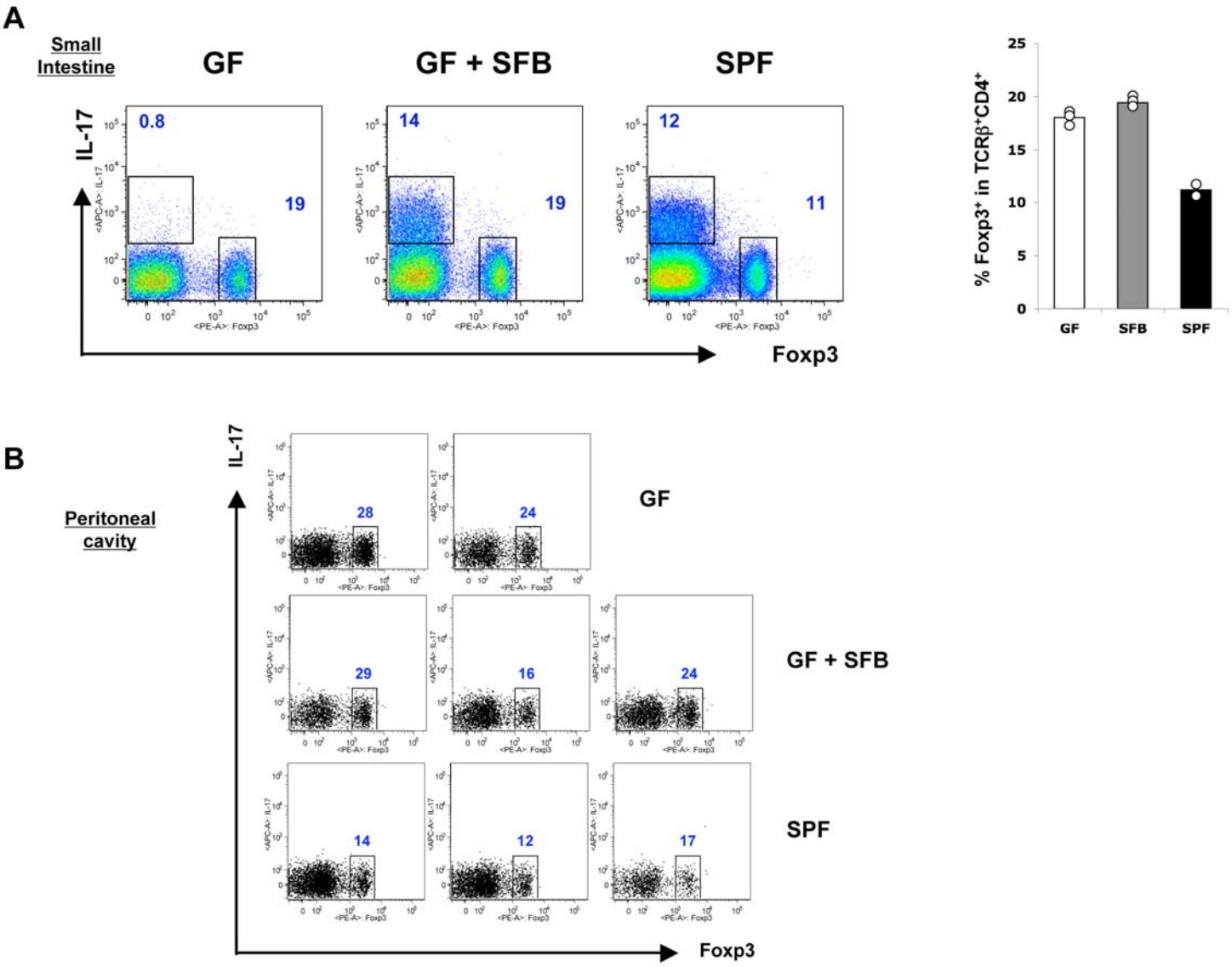

Figure S8. SFB colonization does not affect Foxp3 expression

A. 6 week old Swiss-Webster germ-free (GF) mice were colonized with SFB from feces of SFB-mono mice as described in Methods. SI LPL were prepared 10 days later and analyzed for Foxp3 and IL-17 expression. Plots represent individual mice and are gated on $TCR\beta^{+}CD4^{+}$ lymphocytes. Data from all animals from one of several experiments are plotted on the right.

B. 6 week old Swiss-Webster germ-free (GF) mice were colonized with SFB from feces of SFB-mono mice as described in Methods. Peritoneal cavity mononuclear cells were prepared 3 weeks later and analyzed for Foxp3 and IL-17 expression. Plots represent individual mice and are gated on $TCR\beta^{+}CD4^{+}$ lymphocytes.

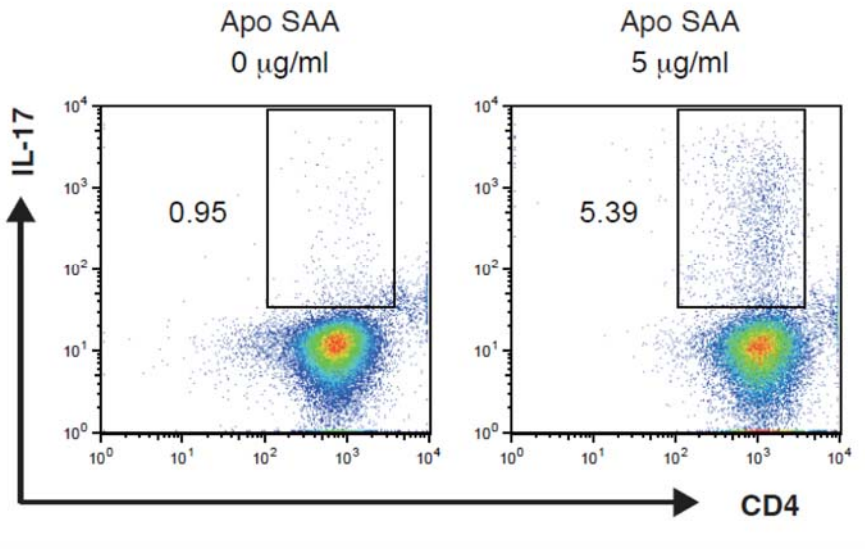

Figure S9. Enhancement of Th17 differentiation by SAA
Splenic $CD4^+$ T cells were purified from OT-II transgenic mice by MACS, and cocultured in 24-well plates at 2 x 10^5 cells/well with lamina propria $CD11c^+$ cells (1 x 10^5 cells/well) in the presence of OVA peptide (OVA323-339) with or without recombinant human SAA (5 μg/ml, Peprotech, cat# 300-13) for 4 days. T cells were restimulated with PMA and ionomycin for 3 hr, and examined for expression of CD4 and IL-17 by FACS. Numbers represent the percentage of $IL\text{-}17^+$ cells among $CD4^+$ T cells.

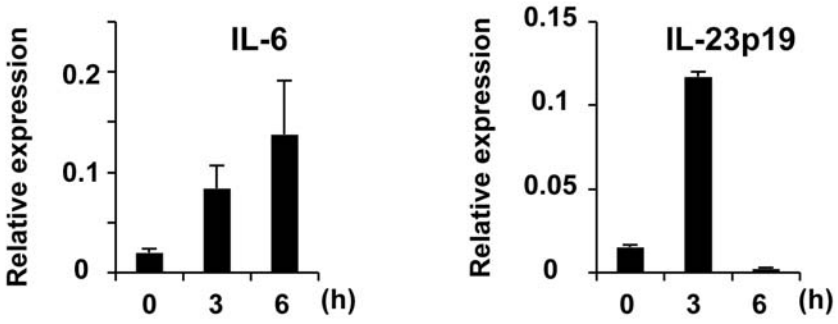

Figure S10. SAA induces IL-6 and IL-23 expression from intestinal DCs
Small intestinal CD11c+ cells were plated in 24-well plates at 2 x 10^5 cells/well, stimulated with 5 μg/ml recombinant Apo-SAA for the indicated times, and real-time RT-PCR performed. Results were normalized to expression of GAPDH mRNA. Cultures were performed in duplicate wells and data shown as the mean +/- SD.

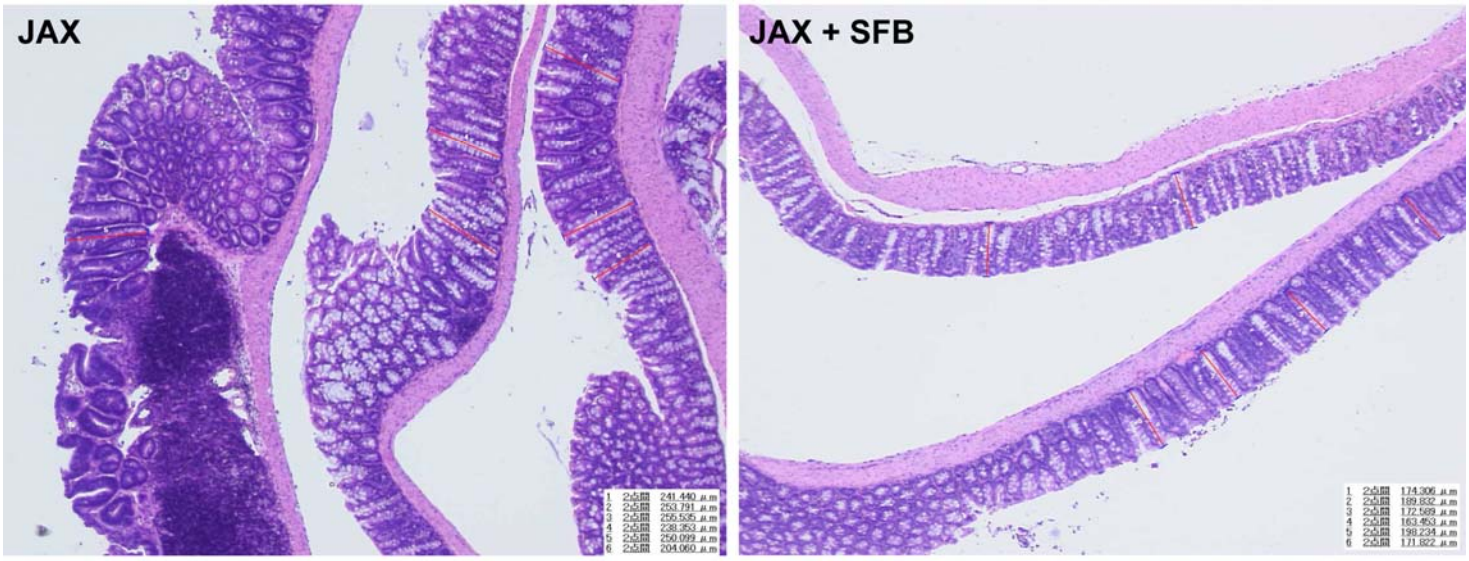

Figure S11. SFB colonization decreases crypt hyperplasia after infection with *Citrobacter rodentium*
IQI GF mice colonized with Jackson microbiota (Jax) or Jax+SFB were orally infected with 2 x 10^9 CFU of *C. rodentium*, and the colons were harvested at day 8 after infection. Representative H&E sections demonstrating the lower degree of epithelial hyperplasia in the presence of SFB and the way crypt length was scored (length of red bars).

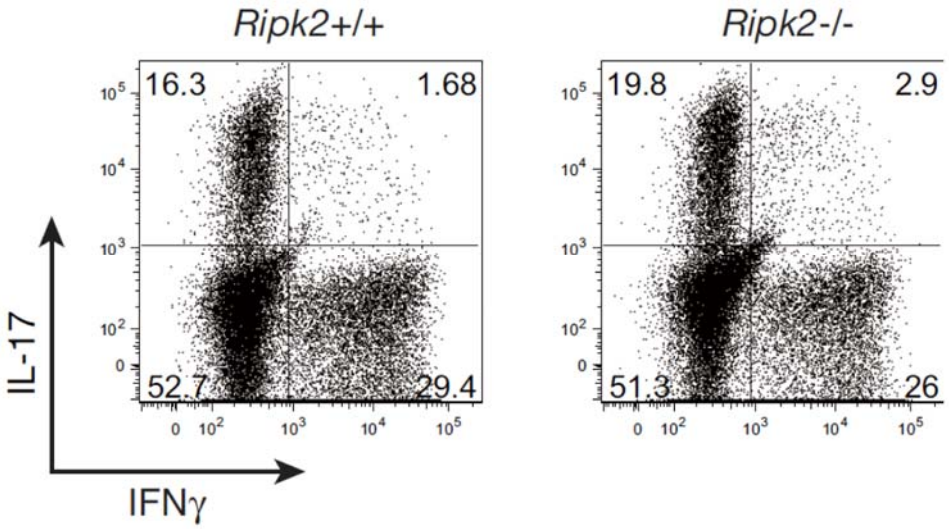

Figure S12. NOD signaling is not required for Th17 cell differentiation in the LP
SI LPL were isolated from RIP2-KO mice and WT littermates and analyzed for intracellular cytokines. Plots represent individual mice and are gated on $TCR\beta^+CD4^+$ lymphocytes. RIP2-KO mice were kindly provided by Genhong Cheng and Paul W. Dempsey of University of California, San Diego, California.